LHCb-CONF-2022-001
April 19, 2022

Modification of $\chi_{c1}(3872)$ and $\psi(2S)$ production in pPb collisions at $\sqrt{s_{NN}} = 8.16\,\text{TeV}$

LHCb collaboration[†]

Abstract

Production of the exotic state $\chi_{c1}(3872)$ is measured in pPb collisions at both forward and backward rapidity by the LHCb experiment. Comparisons with the charmonium state $\psi(2S)$ suggest that the $\chi_{c1}(3872)$ state experiences different dynamics in the nuclear medium than conventional hadrons. This first measurement of the production of an exotic hadron in pPb collisions provides new constraints on models of $\chi_{c1}(3872)$ structure and models of hadron production and transport in nuclear collisions.

[†]Conference report prepared for Quark Matter 2022, Krakow, Poland, April 4-10, 2022.
Contact author: J. Matthew Durham, durham@lanl.gov.

The study of exotic hadrons with more than three valence quarks is a highly active area of quantum chromodynamics. Dozens of exotic states have been discovered in the last 20 years, and various exotic models such as compact tetraquarks, hadronic molecules, hadrocharmonia, and other structures have been proposed in attempts to explain their various properties (see Ref. [1] for a recent review). However, to date, there is no general consensus on the nature of the first discovered and most well-studied exotic hadron, the $\chi_{c1}(3872)$ state.

Most existing measurements of the properties of exotic hadrons utilize their production in the decays of hadrons containing b quarks. These decays provide well-defined initial conditions, and many sources of background can be efficiently rejected using the relatively long lifetime of b hadrons. However, exotic hadrons can also be produced promptly at the interaction point of hadronic collisions, where they can interact with other particles produced in the event. In collisions using beams of nuclei, the exotic hadrons can also interact with the nuclear remnant and are subject to the effects of quark-gluon plasma. The response of the exotic hadrons to these effects provides new ways to constrain their properties, which are not accessible via studies of b decays.

Previous LHCb measurements in pp collisions showed a significant decrease in the ratio of prompt $\chi_{c1}(3872)$ to $\psi(2S)$ cross-sections, $\sigma_{\chi_{c1}(3872)}/\sigma_{\psi(2S)}$, with increasing charged-particle multiplicity [2]. These data were interpreted in terms of breakup of the $\chi_{c1}(3872)$ hadrons due to interactions with comoving particles produced in the event, for both compact and molecular models of $\chi_{c1}(3872)$ structure [3, 4]. The CMS collaboration has measured the $\sigma_{\chi_{c1}(3872)}/\sigma_{\psi(2S)}$ ratio in PbPb collisions, and found that the ratio is enhanced relative to pp collisions, although significant uncertainties on that measurement preclude drawing firm conclusions [5]. Statistical hadronization models predict that $\chi_{c1}(3872)$ production is significantly enhanced in PbPb collisions at the LHC [6, 7]. Calculations based on quark coalescence show that production rates of $\chi_{c1}(3872)$ hadrons in AA collisions are sensitive to its structure. In these models, production of compact tetraquarks is expected to be greatly enhanced over hadronic molecules [8, 9]. However, a recent transport calculation reaches the opposite conclusion [10]. Late stage interactions in the hadron gas phase of a heavy-ion collision can also affect the observed yields [11]. It is currently unknown where the crossover between the suppressing effects of breakup and the enhancing effects of coalescence may occur.

Collisions of protons with Pb nuclei provide an intermediary between the relatively small pp collision system and the large PbPb system, and can thereby shed light on the interplay of various enhancement and suppression mechanisms. Calculations of tetraquark production in pPb collisions have predicted that the $\chi_{c1}(3872)$ cross-section could be enhanced relative to pp collisions, due to a higher rate of double-parton scattering [12]. An increase of double-parton scattering in pPb collisions relative to pp collisions has since been measured by LHCb [13]. An enhancement of proton production relative to pions and kaons has been observed in dAu and pPb collisions [14–16], which can be explained by coalescence of three quarks into baryons versus two quarks into mesons [17–19]. Similarly, an enhancement of charmed baryons relative to charmed mesons has been observed in pp and pPb collisions, relative to expectations from e^+e^- collisions [20, 21], which may be explained by quark coalescence [22]. These coalescence effects could be even more pronounced for four-quark states, which have never been measured in pA collisions. Therefore, in addition to providing new information on the $\chi_{c1}(3872)$ structure, measurements in pPb collisions can provide new tests of models of particle transport and

hadronization in nuclear collisions, in a new range of number of constituent quarks.

This note describes the first measurements of the prompt production of the exotic state $\chi_{c1}(3872)$ relative to the conventional charmonium state $\psi(2S)$ in pPb collisions. Both the $\chi_{c1}(3872)$ and $\psi(2S)$ hadrons are reconstructed through their decays to $J/\psi\pi^+\pi^-$, where the J/ψ subsequently decays to a pair of oppositely charged muons. These measurements use pp and pPb collision data. The pp data is collected by the LHCb experiment at a center-of-mass energy of 8 TeV, corresponding to an integrated luminosity of about 2 fb^{-1}. The pPb data is collected in two configurations. In the forward configuration, denoted pPb, the proton beam is directed into the LHCb spectrometer and measurements cover the rapidity interval $1.5 < y < 4$, where y is measured in the center-of-mass frame of the collision system. In the backward configuration, denoted Pbp, the Pb beam travels into the spectrometer and the resulting rapidity coverage is $-5 < y < -2.5$. The pPb and Pbp data sets considered here were recorded at a center-of-mass energy of 8.16 TeV per nucleon and correspond to integrated luminosities of about 12.5 nb^{-1} and 19.3 nb^{-1}, respectively.

The LHCb detector is a single-arm forward spectrometer, described in detail in Refs. [23, 24]. Events considered in this analysis are selected with a series of triggers which retain events containing the decay $J/\psi \to \mu^+\mu^-$. Muon candidates are required to have total momentum $p > 3\,\text{GeV}/c$ and transverse momentum $p_\text{T} > 650\,\text{MeV}/c$, and to penetrate all of the muon system's hadron absorbers. The dimuon invariant mass spectrum is fit, and candidate J/ψ mesons are formed from pairs of oppositely charged muon candidates that have an invariant mass within three standard deviations around the mean of the J/ψ peak. Charged pion candidates are required to have $p > 3\,\text{GeV}/c$, $p_\text{T} > 500\,\text{MeV}/c$, and are identified by the response of the ring-imaging Cherenkov detectors. Combinations of $\mu^+\mu^-\pi^+\pi^-$ candidates that form a good quality common vertex are retained, and the tracks are refit with kinematic constraints that constrain the $\mu^+\mu^-$ invariant mass to the known J/ψ mass, and require all four tracks to originate from a common vertex. The decay kinematics are required to satisfy $M_{J/\psi\pi^+\pi^-} - M_{J/\psi} - M_{\pi^+\pi^-} < 300\,\text{MeV}/c^2$, which reduces combinatorial backgrounds while retaining signal. The resulting $J/\psi\pi^+\pi^-$ candidates are required to have $p_\text{T} > 5\,\text{GeV}/c$.

The $\chi_{c1}(3872)$ and $\psi(2S)$ signals of interest for this measurement are produced promptly at the collision vertex, where they are subject to interactions with other particles in the event. The pseudo decay-time t_z is used to select promptly produced signal candidates and reject those produced in decays of b hadrons. This variable is defined as

$$t_z \equiv \frac{(z_\text{decay} - z_\text{PV}) \times M}{p_z}, \tag{1}$$

where $z_\text{decay} - z_\text{PV}$ is the difference between the positions of the reconstructed vertex of the $J/\psi\pi^+\pi^-$ candidate and the associated collision vertex along the beam axis, M is the mass of the reconstructed signal candidate, and p_z is the candidate's momentum along the beam axis. A requirement of $t_z < 0.1$ ps is applied. The data and simulations show that this retains more than 99% of the prompt signals, while rejecting $\sim 80\%$ of the signals produced away from the primary vertex in decays of b hadrons. The resulting $J/\psi\pi^+\pi^-$ invariant mass spectra from pp, pPb, and Pbp collisions are shown in Fig. 1.

The $J/\psi\pi^+\pi^-$ mass distributions are fit to extract the ratio of $\chi_{c1}(3872)$ to $\psi(2S)$ signal yields. In the fit, the $\chi_{c1}(3872)$ line shape is represented by a Gaussian function, while the $\psi(2S)$ peak is represented by the sum of two Crystal Ball functions, with a

low- and high-mass tail [25]. The background is studied by constructing the invariant mass spectrum of $J/\psi\pi^{\pm}\pi^{\pm}$ combinations using like-sign dipions, and is well represented by a third-order Chebychev polynomial in all data sets. When fitting the pPb and Pbp samples, the $\chi_{c1}(3872)$ and $\psi(2S)$ line shapes are fixed to the shapes determined by fitting the relatively high-statistics pp sample, while their normalizations and the background parameters are allowed to float. The $\chi_{c1}(3872)$ signal yields with their statistical uncertainties are determined to be 137±37 and 108±40 for the pPb and Pbp data sets, respectively. The corresponding $\psi(2S)$ yields are 343±32 and 190±30 for the pPb and Pbp data sets. Variations of the fit functions that converge to meaningful values in the pp data give negligible variations in the yields extracted from the pPb and Pbp

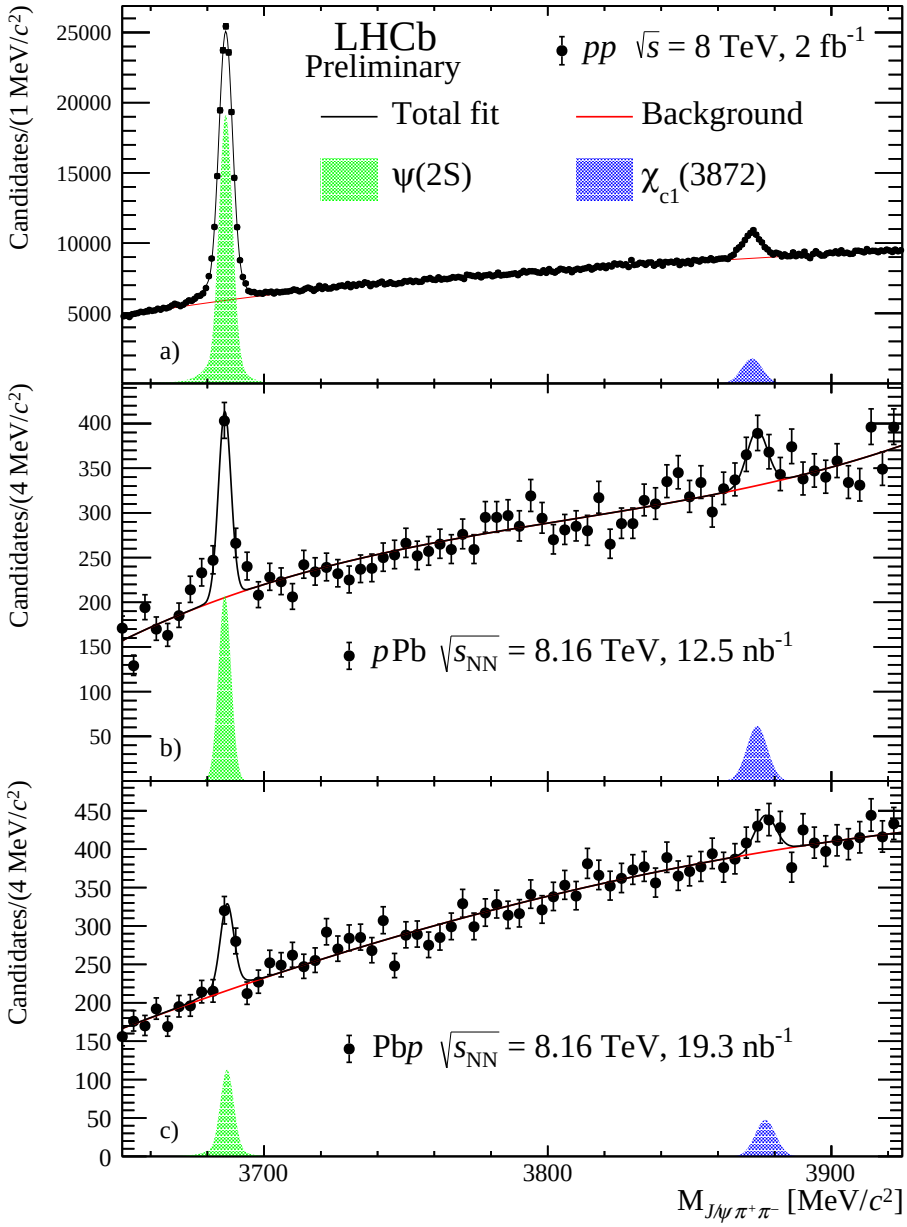

Figure 1: The $J/\psi\pi^{+}\pi^{-}$ invariant mass spectra measured in a) pp, b) pPb, and c) Pbp collisions, with fit projections overlaid.

data sets. Fit projections are shown overlaid on the data in Fig. 1.

Simulation is required to model the effects of the detector acceptance and the imposed selection requirements. In the simulation, pp collisions are generated using Pythia [26] with a specific LHCb configuration [27]. Decays of unstable particles are described by EvtGen [28]. The interaction of the generated particles with the detector, and its response, are implemented using the Geant4 toolkit [29] as described in Ref. [30]. The $p_{\rm T}$ distributions of the simulated $\chi_{c1}(3872)$ and $\psi(2S)$ decays are weighted to match distributions extracted from the data using the *sPlot* method [31].

The ratio of cross-sections for prompt $\sigma_{\chi_{c1}(3872)}/\sigma_{\psi(2S)}$ times their branching fractions $\mathcal{B}$ to $J/\psi\pi^+\pi^-$ is given by

$$\frac{\sigma_{\chi_{c1}(3872)}(p_{\rm T}>5\,{\rm GeV}/c)}{\sigma_{\psi(2S)}(p_{\rm T}>5\,{\rm GeV}/c)}\times\frac{\mathcal{B}[\chi_{c1}(3872)\to J/\psi\pi^+\pi^-]}{\mathcal{B}[\psi(2S)\to J/\psi\pi^+\pi^-]}= \frac{N_{\chi_{c1}(3872)}}{N_{\psi(2S)}}\times\frac{\epsilon^{\rm acc}_{\psi(2S)}}{\epsilon^{\rm acc}_{\chi_{c1}(3872)}}\times\frac{\epsilon^{\rm trig}_{\psi(2S)}}{\epsilon^{\rm trig}_{\chi_{c1}(3872)}}\times\frac{\epsilon^{\rm reco}_{\psi(2S)}}{\epsilon^{\rm reco}_{\chi_{c1}(3872)}}\times\left[\frac{\epsilon^{\mu^\pm{\rm PID}}_{\psi(2S)}}{\epsilon^{\mu^\pm{\rm PID}}_{\chi_{c1}(3872)}}\right]^2\times\left[\frac{\epsilon^{\pi^\pm{\rm PID}}_{\psi(2S)}}{\epsilon^{\pi^\pm{\rm PID}}_{\chi_{c1}(3872)}}\right]^2 \quad (2)$$

where $N_{\chi_{c1}(3872)}/N_{\psi(2S)}$ is the ratio of signal yields returned by the fit, and the efficiency ratios are discussed below.

The ratio of geometric acceptance for the daughter products $\epsilon^{\rm acc}_{\psi(2S)}/\epsilon^{\rm acc}_{\chi_{c1}(3872)}$ is determined by simulation to be close to one with a systematic uncertainty of 1%, due to the uncertainty on the weights applied to the simulation to match the data. The ratio of trigger efficiencies $\epsilon^{\rm trig}_{\psi(2S)}/\epsilon^{\rm trig}_{\chi_{c1}(3872)}$ is determined from data to be consistent with one within an uncertainty of 2%, using techniques described in Ref. [32], where the uncertainty comes from statistical uncertainties on the data sample. The ratio of reconstruction efficiencies $\epsilon^{\rm reco}_{\psi(2S)}/\epsilon^{\rm reco}_{\chi_{c1}(3872)}$ is determined to be 0.67 ± 0.12 (0.61 ± 0.19) for pPb (Pbp) collisions, where the uncertainty is due to the statistical uncertainty on the $p_{\rm T}$ distributions of signals extracted from the data. The deviation of this term from one is due to the difference in the kinematics of $\chi_{c1}(3872)$ and $\psi(2S)$ decays. The dipions from $\psi(2S)\to J/\psi\pi^+\pi^-$ decays proceed directly to the final-state and have masses between $\sim$300 and 600 MeV/c, while the dipions from $\chi_{c1}(3872)\to J/\psi\pi^+\pi^-$ decays are dominated by an intermediate $\rho(770)^0$ state with higher mass and are reconstructed with a higher efficiency [33]. The ratios of muon and pion particle identification efficiencies, $\epsilon^{\mu^\pm{\rm PID}}_{\psi(2S)}/\epsilon^{\mu^\pm{\rm PID}}_{\chi_{c1}(3872)}$ and $\epsilon^{\pi^\pm{\rm PID}}_{\psi(2S)}/\epsilon^{\pi^\pm{\rm PID}}_{\chi_{c1}(3872)}$, are determined using calibration samples of identified particles from the data to be consistent with one, with uncertainties of 1% due to the finite size of the calibration sample.

The resulting ratios of cross-sections are $0.27\pm0.08\pm0.05$ in pPb and $0.36\pm0.15\pm0.11$ in Pbp, where the first and second uncertainties are statistical and systematic, respectively. These ratios are shown in Fig. 2, along with multiplicity-integrated LHCb data from pp collisions [2], and CMS data from PbPb collisions [5], which is measured over the rapidity interval $|y|<0.9$ and in a significantly higher $p_{\rm T}$ range. In this ratio, some effects that modify charm production in nuclear collisions, such as modification of the nuclear parton distribution function, largely cancel, leaving final-state effects as the dominant modification mechanism. There is an increase in the ratio as the system size increases, which may be due to a combination of effects. It has been observed that $\psi(2S)$ production is suppressed in pA collisions [34–40], which would drive the ratio upwards even if no final-state effects are present on the $\chi_{c1}(3872)$ resonance. However, given that pp collisions

show a decreasing trend with multiplicity [2], the increase of the ratio may indicate that the hadronic densities achieved in the pPb an Pbp configurations allow quark coalescence to become the dominant mechanism affecting $\chi_{c1}(3872)$ production. Future measurements of the nuclear modification factor of $\chi_{c1}(3872)$ and $\psi(2S)$, which are in progress at LHCb, can clarify these effects.

In summary, the LHCb collaboration has produced the first measurement of the exotic state $\chi_{c1}(3872)$ in pPb collisions. The increase of the ratio of cross-sections $\sigma_{\chi_{c1}(3872)}/\sigma_{\psi(2S)}$ from pp to pPb to PbPb collisions may indicate that the exotic $\chi_{c1}(3872)$ hadron experiences different dynamics in the nuclear medium than the conventional charmonium state $\psi(2S)$. These measurements can provide new constraints on the allowed configurations of quarks inside hadrons, as well as models of parton transport and hadronization in nuclear collisions.

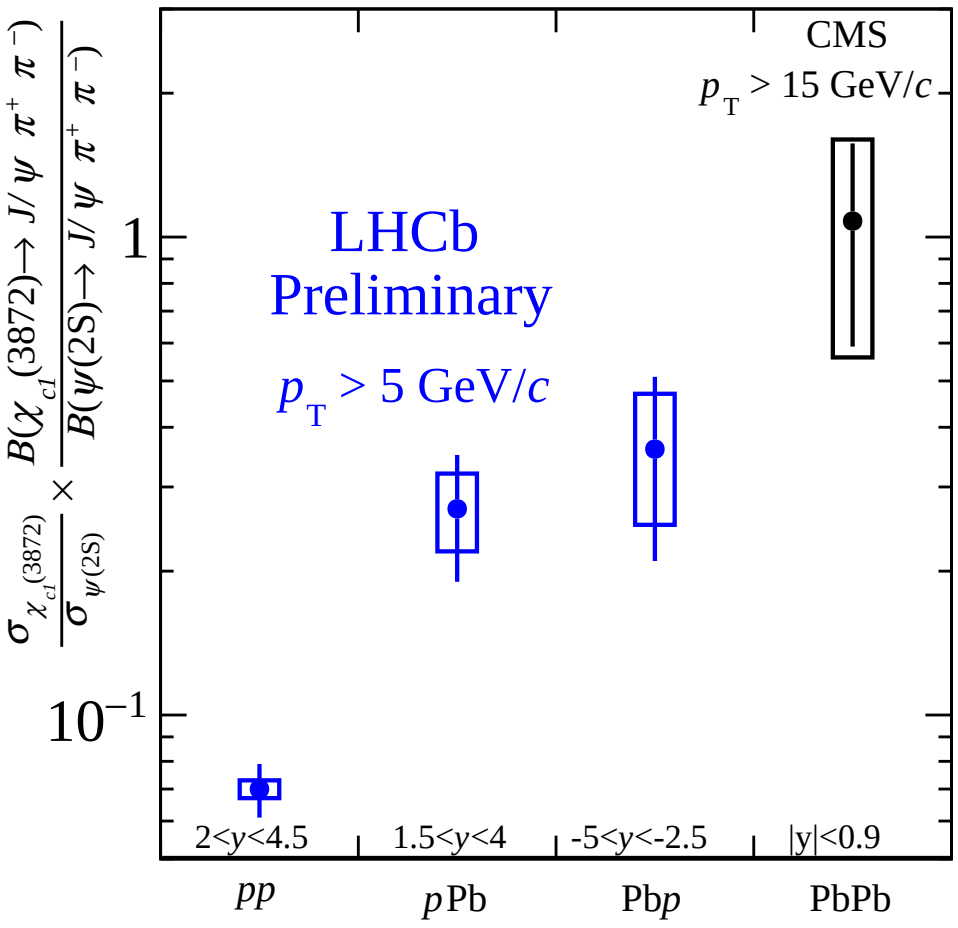

Figure 2: The ratio of $\chi_{c1}(3872)$ to $\psi(2S)$ cross-sections in the $J/\psi\pi^+\pi^-$ decay channel, measured in pp [2], pPb, Pbp, and PbPb [5] collisions. The error bars (boxes) represent the statistical (systematic) uncertainties on the ratio.

Acknowledgements

We express our gratitude to our colleagues in the CERN accelerator departments for the excellent performance of the LHC. We thank the technical and administrative staff at the LHCb institutes. We acknowledge support from CERN and from the national agencies: CAPES, CNPq, FAPERJ and FINEP (Brazil); MOST and NSFC (China); CNRS/IN2P3 (France); BMBF, DFG and MPG (Germany); INFN (Italy); NWO (Netherlands); MNiSW and NCN (Poland); MEN/IFA (Romania); MSHE (Russia); MICINN (Spain); SNSF and SER (Switzerland); NASU (Ukraine); STFC (United Kingdom); DOE NP and NSF (USA). We acknowledge the computing resources that are provided by CERN, IN2P3 (France), KIT and DESY (Germany), INFN (Italy), SURF (Netherlands), PIC (Spain), GridPP (United Kingdom), RRCKI and Yandex LLC (Russia), CSCS (Switzerland), IFIN-HH (Romania), CBPF (Brazil), PL-GRID (Poland) and NERSC (USA). We are indebted to the communities behind the multiple open-source software packages on which we depend. Individual groups or members have received support from ARC and ARDC (Australia); AvH Foundation (Germany); EPLANET, Marie Skłodowska-Curie Actions and ERC (European Union); A*MIDEX, ANR, Labex P2IO and OCEVU, and Région Auvergne-Rhône-Alpes (France); Key Research Program of Frontier Sciences of CAS, CAS PIFI, CAS CCEPP, Fundamental Research Funds for the Central Universities, and Sci. & Tech. Program of Guangzhou (China); RFBR, RSF and Yandex LLC (Russia); GVA, XuntaGal and GENCAT (Spain); the Leverhulme Trust, the Royal Society and UKRI (United Kingdom).

References

[1] S. L. Olsen, T. Skwarnicki, and D. Zieminska, *Nonstandard heavy mesons and baryons: experimental evidence*, Rev. Mod. Phys. **90** (2018) 015003, arXiv:1708.04012.

[2] LHCb collaboration, R. Aaij *et al.*, *Observation of multiplicity dependent* $\chi_{c1}(3872)$ *and* $\psi(2S)$ *production in pp collisions*, Phys. Rev. Lett. **126** (2021) 092001, arXiv:2009.06619.

[3] A. Esposito *et al.*, *The nature of X(3872) from high-multiplicity pp collisions*, Eur. Phys. J. **C81** (2021) 669, arXiv:2006.15044.

[4] E. Braaten, L.-P. He, K. Ingles, and J. Jiang, *Production of* $X(3872)$ *at high multiplicity*, Phys. Rev. **D103** (2021) L071901, arXiv:2012.13499.

[5] CMS collaboration, A. M. Sirunyan *et al.*, *Evidence for X(3872) in Pb-Pb collisions and studies of its prompt production at* $\sqrt{s_{NN}} = 5.02\ TeV$, Phys. Rev. Lett. **128** (2022) 032001, arXiv:2102.13048.

[6] S. Cho and S. H. Lee, *Production of multicharmed hadrons by recombination in heavy ion collisions*, Phys. Rev. C **101** (2020) 024902, arXiv:1907.12786.

[7] A. Andronic *et al.*, *Transverse momentum distributions of charmonium states with the statistical hadronization model*, Phys. Lett. **B797** (2019) 134836, arXiv:1901.09200.

[8] ExHIC collaboration, S. Cho *et al.*, *Multi-quark hadrons from Heavy Ion Collisions*, Phys. Rev. Lett. **106** (2011) 212001, arXiv:1011.0852.

[9] ExHIC collaboration, S. Cho *et al.*, *Studying Exotic Hadrons in Heavy Ion Collisions*, Phys. Rev. C **84** (2011) 064910, arXiv:1107.1302.

[10] B. Wu, X. Du, M. Sibila, and R. Rapp, $X(3872)$ *transport in heavy-ion collisions*, Eur. Phys. J. **A57** (2021) 122, arXiv:2006.09945, [Erratum: Eur.Phys.J.A 57, 314 (2021)].

[11] L. M. Abreu *et al.*, $X(3872)$ *production and absorption in a hot hadron gas*, Phys. Lett. B **761** (2016) 303, arXiv:1604.07716.

[12] F. Carvalho and F. S. Navarra, *Nuclear effects on tetraquark production by double parton scattering*, EPJ Web Conf. **137** (2017) 06004.

[13] LHCb collaboration, R. Aaij *et al.*, *Observation of enhanced double parton scattering in proton-lead collisions at* $\sqrt{s_{NN}} = 8.16$ *TeV*, Phys. Rev. Lett. **125** (2020) 212001, arXiv:2007.06945.

[14] STAR collaboration, J. Adams *et al.*, *Pion, kaon, proton and anti-proton transverse momentum distributions from* $p + p$ *and* $d+$ *Au collisions at* $\sqrt{s_{NN}} = 200\,GeV$, Phys. Lett. **B616** (2005) 8, arXiv:nucl-ex/0309012.

[15] PHENIX collaboration, A. Adare *et al.*, *Spectra and ratios of identified particles in Au+Au and d+Au collisions at* $\sqrt{s_{NN}} = 200$ *GeV*, Phys. Rev. **C88** (2013) 024906, arXiv:1304.3410.

[16] ALICE collaboration, J. Adam *et al.*, *Multiplicity dependence of charged pion, kaon, and (anti)proton production at large transverse momentum in p-Pb collisions at* $\sqrt{s_{NN}}$ *= 5.02 TeV*, Phys. Lett. **B760** (2016) 720, arXiv:1601.03658.

[17] R. C. Hwa and C. B. Yang, *Final state interaction as the origin of the Cronin effect*, Phys. Rev. Lett. **93** (2004) 082302, arXiv:nucl-th/0403001.

[18] R. C. Hwa and C. B. Yang, *Proton production in d+Au collisions and the Cronin effect*, Phys. Rev. **C70** (2004) 037901, arXiv:nucl-th/0404066.

[19] F.-l. Shao *et al.*, *Yield ratios of identified hadrons in p+p, p+Pb , and Pb+Pb collisions at energies available at the CERN Large Hadron Collider*, Phys. Rev. **C95** (2017) 064911, arXiv:1703.05862.

[20] ALICE collaboration, S. Acharya *et al.*, *Charm-quark fragmentation fractions and production cross section at midrapidity in pp collisions at the LHC*, Phys. Rev. **D105** (2022) L011103, arXiv:2105.06335.

[21] ALICE collaboration, S. Acharya *et al.*, Λ_c^+ *production and baryon-to-meson ratios in pp and p-Pb Collisions at* $\sqrt{s_{NN}}$*=5.02 TeV at the LHC*, Phys. Rev. Lett. **127** (2021) 202301, arXiv:2011.06078.

[22] S. Plumari *et al.*, *Charmed hadrons from coalescence plus fragmentation in relativistic nucleus-nucleus collisions at RHIC and LHC*, Eur. Phys. J. **C78** (2018) 348, arXiv:1712.00730.

[23] LHCb collaboration, A. A. Alves Jr. *et al.*, *The LHCb detector at the LHC*, JINST **3** (2008) S08005.

[24] LHCb collaboration, R. Aaij *et al.*, *LHCb detector performance*, Int. J. Mod. Phys. **A30** (2015) 1530022, arXiv:1412.6352.

[25] J. Gaiser *et al.*, *Charmonium Spectroscopy from Inclusive psi-prime and J/psi Radiative Decays*, Phys. Rev. **D34** (1986) 711.

[26] T. Sjöstrand, S. Mrenna, and P. Skands, *A brief introduction to PYTHIA 8.1*, Comput. Phys. Commun. **178** (2008) 852, arXiv:0710.3820; T. Sjöstrand, S. Mrenna, and P. Skands, *PYTHIA 6.4 physics and manual*, JHEP **05** (2006) 026, arXiv:hep-ph/0603175.

[27] I. Belyaev *et al.*, *Handling of the generation of primary events in Gauss, the LHCb simulation framework*, J. Phys. Conf. Ser. **331** (2011) 032047.

[28] D. J. Lange, *The EvtGen particle decay simulation package*, Nucl. Instrum. Meth. **A462** (2001) 152.

[29] Geant4 collaboration, J. Allison *et al.*, *Geant4 developments and applications*, IEEE Trans. Nucl. Sci. **53** (2006) 270; Geant4 collaboration, S. Agostinelli *et al.*, *Geant4: A simulation toolkit*, Nucl. Instrum. Meth. **A506** (2003) 250.

[30] M. Clemencic *et al.*, *The LHCb simulation application, Gauss: Design, evolution and experience*, J. Phys. Conf. Ser. **331** (2011) 032023.

[31] M. Pivk and F. R. Le Diberder, *SPlot: a statistical tool to unfold data distributions*, Nucl. Instrum. Meth. **A555** (2005) 356, arXiv:physics/0402083.

[32] S. Tolk, J. Albrecht, F. Dettori, and A. Pellegrino, *Data driven trigger efficiency determination at LHCb*, LHCb-PUB-2014-039, 2014.

[33] CDF collaboration, A. Abulencia *et al.*, *Measurement of the dipion mass spectrum in $X(3872) \to J/\psi\pi^+\pi^-$ decays.*, Phys. Rev. Lett. **96** (2006) 102002, arXiv:hep-ex/0512074.

[34] PHENIX collaboration, A. Adare *et al.*, *Nuclear Modification of ψ', χ_c, and J/ψ Production in d+Au Collisions at $\sqrt{s_{NN}} = 200$ GeV*, Phys. Rev. Lett. **111** (2013) 202301, arXiv:1305.5516.

[35] ALICE collaboration, B. B. Abelev *et al.*, *Suppression of ψ(2S) production in p-Pb collisions at $\sqrt{s_{NN}} = 5.02$ TeV*, JHEP **12** (2014) 073, arXiv:1405.3796.

[36] LHCb collaboration, R. Aaij *et al.*, *Study of $\psi(2S)$ production cross-sections and cold nuclear matter effects in pPb collisions at $\sqrt{s_{NN}} = 5$ TeV*, JHEP **03** (2016) 133, arXiv:1601.07878.

[37] PHENIX collaboration, A. Adare *et al.*, *Measurement of the relative yields of $\psi(2S)$ to $\psi(1S)$ mesons produced at forward and backward rapidity in p+p, p+Al, p+Au, and ^{3}He+Au collisions at $\sqrt{s_{NN}}$ = 200 GeV*, Phys. Rev. **C95** (2017) 034904, arXiv:1609.06550.

[38] CMS collaboration, A. M. Sirunyan *et al.*, *Measurement of prompt $\psi(2S)$ production cross sections in proton-lead and proton-proton collisions at $\sqrt{s_{NN}}$ = 5.02 TeV*, Phys. Lett. **B790** (2019) 509, arXiv:1805.02248.

[39] ALICE collaboration, S. Acharya *et al.*, *Measurement of nuclear effects on ψ(2S) production in p-Pb collisions at $\sqrt{s_{NN}}$ = 8.16 TeV*, JHEP **07** (2020) 237, arXiv:2003.06053.

[40] PHENIX collaboration, U. A. Acharya *et al.*, *Measurement of $\psi(2S)$ nuclear modification at backward and forward rapidity in p + p, p + Al, and p + Au collisions at $\sqrt{s_{NN}}$ = 200 GeV*, arXiv:2202.03863.